

Assessment of the effectiveness of the NSM shear strengthening technique for deep T cross section RC beams

J. Barros ¹, S. Dias ²

¹ISISE, University of Minho, Guimarães, Portugal, barros@civil.uminho.pt

²ISISE, University of Minho, Guimarães, Portugal, sdias@civil.uminho.pt

Keywords: NSM; CFRP; Shear strengthening; Deep beams.

SUMMARY

The effectiveness of the near surface mounted (NSM) technique with carbon fibre reinforced polymer (CFRP) laminates for the shear strengthening of reinforced concrete (RC) beams has been demonstrated during the last decade. Analytical and numerical research indicate that the NSM technique for the shear strengthening of RC beams can be more effective if the CFRP laminates are deeper installed into the slits. However, the depth of the slits is conditioned by the thickness of concrete cover of the lateral faces of the beam. Furthermore, relatively deep slits can only be executed, by maintaining an effective bond transfer length for the CFRP laminates crossing the shear crack, if the beam's cross section is relatively high. Therefore, an experimental program composed of a series of RC beams of relatively high T cross section web, shear strengthened according to the NSM technique with CFRP laminates, was carried out. The experimental program is described and the main results are presented and discussed.

1. INTRODUCTION

Near surface mounted (NSM) technique by using carbon fibre reinforced polymer (CFRP) laminates introduced into thin slits open on the lateral surfaces of reinforced concrete (RC) beams has been proved to be very effective for the shear strengthening of this type of structural elements [1-3]. The laminates are bonded to the surrounding concrete by using epoxy adhesive, and the depth of the slits is limited to the concrete cover of the beam's lateral faces, which, in general, does not exceed 30 mm.

A recent analytical model has demonstrated that the deeper the laminate is installed into the core of the beam's web, the more effective is the NSM technique with CFRP laminates for the shear strengthening [4]. The model assumes that the possible failure modes governing the strengthening effectiveness of a NSM laminate comprise loss of bond (debonding), concrete semi-conical tensile fracture, mixed shallow-semi-cone-plus-debonding, and laminate tensile fracture. The semi-conical geometry for the concrete tensile fracture failure mode is assumed formed when the axis of the laminate is assumed positioned at the surface of the beam's lateral face. According to the theoretical fundamentals of this model, if the laminate is positioned deeper into the core of the beam's web, the concrete fracture failure surface has higher fracture area than the one corresponding to the semi-cone, resulting higher resisting concrete fracture force and, consequently, higher shear strengthening effectiveness for the NSM technique. Pullout tests with NSM systems have also demonstrated that the deeper is the laminate installed into the slit the larger is the maximum pullout force [5]. Taking into account these experimental, analytical and numerical evidences about the benefits of installing the CFRP laminates as deeper as possible, an experimental program with T cross section RC beams was carried out, where the depth of the beam's web is high enough to allow the installation of CFRP laminates into relatively deep slits executed above the longitudinal tensile bars, and with enough bond

length for the laminates. The present paper describes the experimental program and presents and discusses the relevant results.

2. EXPERIMENTAL PROGRAM

The experimental program is composed of a reference beam (Fig. 1) and four NSM shear strengthened beams (Fig. 2). Fig. 1 represents the T cross section geometry and the steel reinforcement detailing for the series of beams, as well as the loading configuration and support conditions. The adopted reinforcement systems were designed to assure shear failure mode for all the tested beams. To localize the shear failure in only one of the beam shear spans, a three point loading configuration with a distinct length for the beam shear spans was selected, as shown in Fig. 1. The monitored beam span (a) is 2.5 times the effective depth of the beam ($a/d=2.5$), since, according to the available research [6], this is the minimum value that assures a negligible arch effect. To avoid shear failure in the b beam span, steel stirrups of 6 mm diameter at a spacing of 112 mm ($\phi 6@112\text{mm}$) were applied in this span. To prevent brittle spalling of the concrete cover at the supports, the beam ends were strengthened by confining the concrete with a two-directional cage of $\phi 6@65\text{mm}$ horizontal stirrups and $\phi 10@50\text{mm}$ vertical stirrups (Fig. 1). To overcome the difficulties of bending the $\phi 32$ mm longitudinal tensile bars, their ends were welded to a steel plate.

The differences between the tested beams are restricted to the shear reinforcement systems applied in the a beam span. The reference beam is designated as 3S-R (three steel stirrups in the a shear span, 3S, leading a steel shear reinforcing ratio, ρ_{sw} , of 0.09%), while the following different NSM strengthening configurations were adopted for the other four beams that also include 3 steel stirrups in the a shear span (Fig. 2 and Table 1):

3S-4LI-S2 - four CFRP laminates of type 2 (with a cross section of $1.4 \times 20 \text{ mm}^2$) per face, inclined at 52 degrees with respect to the longitudinal axis of the beam ($\theta_f = 52^\circ$), and installed from the bottom surface of the flange to the bottom tensile surface of the beam's web, i.e., bridging the total lateral surfaces of the beam's web; each CFRP laminate was installed in the out part of a slit of a depth of 21 mm executed on the beam's web lateral surfaces. The length of each laminate was 634 mm;

3S-4LI-P2 - four CFRP laminates of type 2 (with a cross section of $1.4 \times 20 \text{ mm}^2$) per face, inclined at 52 degrees with respect to the longitudinal axis of the beam ($\theta_f = 52^\circ$), and installed from the bottom surface of the flange up to 10 mm above the top surface of the longitudinal tensile steel reinforcement. Each CFRP laminate was installed in the deeper part of a slit of a depth of 35 mm from the surface of the beam's web lateral surfaces. The length of each laminate was 527 mm;

3S-4LI4LI-SP1 - eight CFRP laminates of type 1 (with a cross section of $1.4 \times 10 \text{ mm}^2$) per face, inclined at 52 degrees with respect to the longitudinal axis of the beam ($\theta_f = 52^\circ$). The configuration of the slits executed on the 3S-4LI4LI-SP1 beam combines the configurations of the beams 3S-4LI-P2 and 3S-4LI-S2. In each slit, with a depth of 35mm, was installed one laminate as deeper as possible and one laminate as superficial as possible.

3S-4LI4LV-SP1 - eight CFRP laminates of type 1 (with a cross section of $1.4 \times 10 \text{ mm}^2$) per face, four of them inclined at 52 degrees with respect to the longitudinal axis of the beam ($\theta_f = 52^\circ$) and bridging the total lateral surfaces of the beam's web (the length of each inclined laminate was 634 mm), while the other four laminates were installed in vertical slits executed from the bottom surface of the web up to 10 mm above the top surface of the longitudinal tensile steel reinforcement (the length of each vertical laminate was 432 mm). The vertical laminates were installed as deeper as possible into a slit of a depth of 35 mm from the surface of the beam's web lateral surfaces. The inclined laminates were installed as external as possible into a slit of a depth of 15 mm executed on the beam's web lateral surfaces.

Laminates of $1.4 \times 10 \text{ mm}^2$ cross section were used in the strengthening configurations of the 3S-4LI4LI-SP1 and 3S-4LI4LV-SP1 beams in order to assure a shear strengthening ratio for these beams ($\rho_f = 0.101\%$) similar to the ones applied in the 3S-4LI-S2 and 3S-4LI-P2 beams ($\rho_f = 0.113\%$), where laminates of $1.4 \times 20 \text{ mm}^2$ cross section were applied. The configuration adopted for the CFRP laminates avoided any type of injury in the steel reinforcements during the execution of the slits. The details of the shear strengthening configurations are indicated in Table 1. A general analysis of the data of Table 1 shows that the tested beams had a percentage of longitudinal tensile steel bars (ρ_{sl}) of

2%, a percentage of steel stirrups (ρ_{sw}) of 0.09%, and a percentage of NSM CFRP laminates ranging from 0.101% to 0.113%.

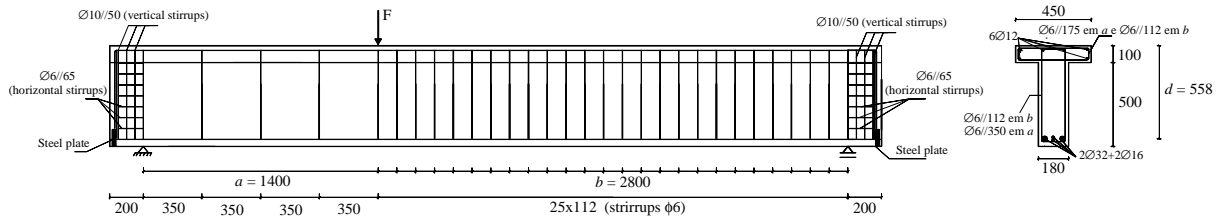


Figure 1: Geometry of the reference beam (3S-R), steel reinforcements common to all beams, support and load conditions (dimensions in mm).

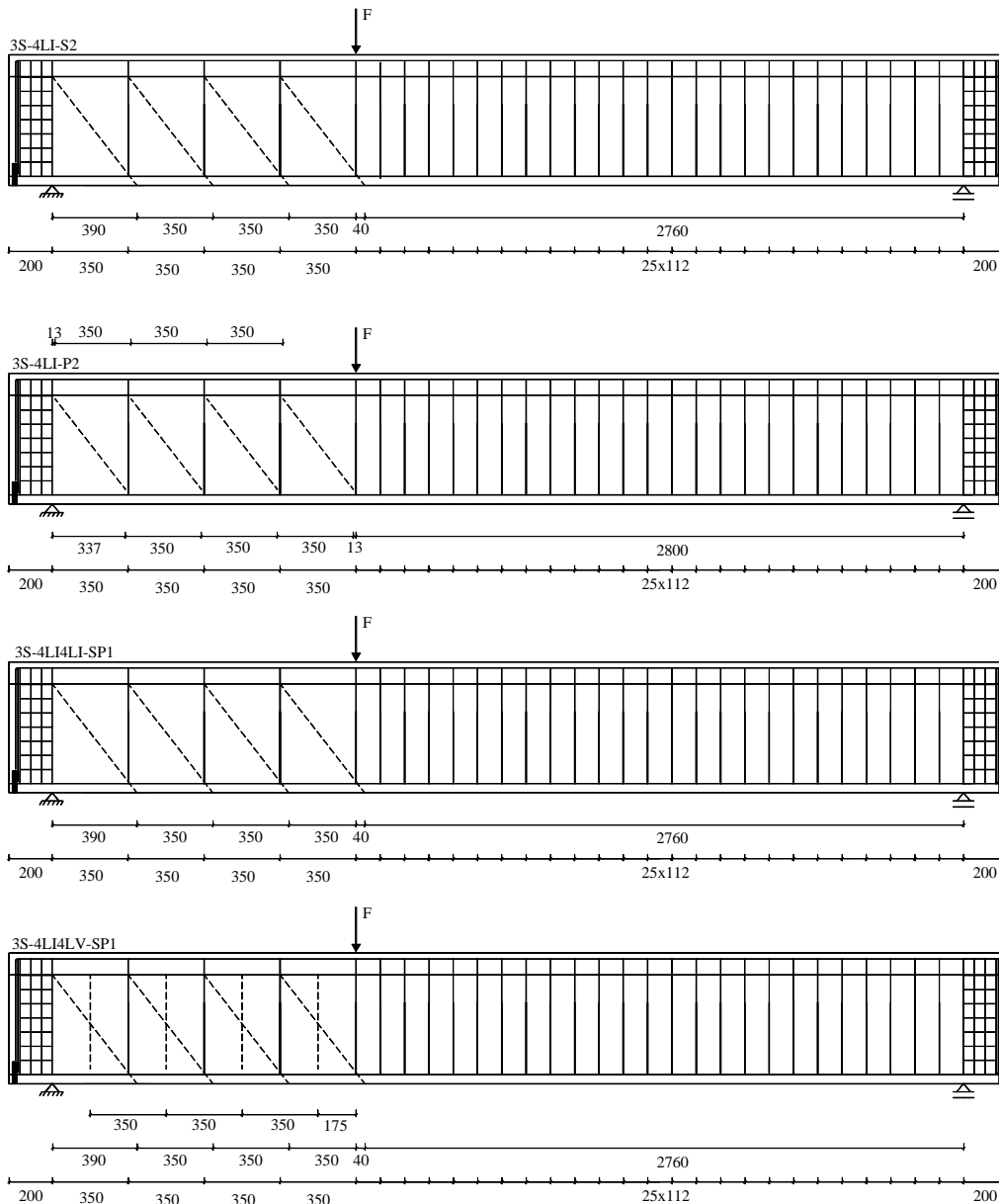


Figure 2: NSM shear strengthening configurations (CFRP laminates at dashed lines; dimensions in mm).

All the NSM shear strengthened beams were executed with a concrete that at the age of the tests of the beams (371 days) presented an average compressive strength (f_{cm}) of 40.1 MPa, measured in cylinders of 150 mm diameter and 300 mm height. At the age of the test of the beam 3S-R (120 days) the value

of f_{cm} was 36.4 MPa. The average value of the yield stress of the steel bars of 6, 12, 16 and 32 mm diameter was 556.1, 566.6, 560.8 and 654.5 MPa, respectively, while average value of the ultimate stress for these corresponding bars was: 682.6, 661.6, 675.0 and 781.9 MPa.

CFK 150/2000 S&P laminates were used in the present experimental research. The tensile properties of both types of laminates (with cross section of $1.4 \times 10 \text{ mm}^2$, type 1, and $1.4 \times 20 \text{ mm}^2$, type 2) were evaluated following the recommendations of ISO 527-5 (1997) [7]. The average value of the tensile strength (f_{tu}), elasticity modulus (E_f), and ultimate strain (ϵ_{fu}) of type 1 CFRP laminate was 3009.3 MPa, 169.2 GPa and 17.8‰, while type 2 CFRP laminate presented the following average values for the corresponding parameters: 2577.2 MPa, 166 GPa and 15.5‰.

S&P Resin 220 epoxy adhesive was used to bond the CFRP laminates to the concrete substrate. The instantaneous and long term tensile behaviour of this adhesive was investigated by Costa and Barros [8]. At 3 days, at which the elasticity modulus ($E_{0.5-2.5\%}$) has attained a stabilized value, the tensile strength and the $E_{0.5-2.5\%}$, determined according to the ISO 527-2 recommendations [9], was about 20 MPa and 7 GPa, respectively.

Table 1: General information about the series of tested RC beams.

Beam	ρ_{sl} [%] ⁽¹⁾	ρ_f [%] ⁽²⁾	θ_f [°]	ρ_{sw} [%] ⁽³⁾	f_{cm} [MPa]	a/d
3S-4LI-S2	2.0	0.113	52	0.09	40.1	2.5
3S-4LI-P2		0.113	52			
3S-4LI4LI-SP1		0.113	52			
3S-4LI4LV-SP1		0.101	52/90			

(1) The percentage of the longitudinal tensile reinforcement was obtained from $\rho_{sl} = (A_{sl} / (b_w \times d)) \times 100$ where A_{sl} is the cross sectional area of the longitudinal tensile steel reinforcement (see Fig. 1), $b_w = 180 \text{ mm}$ is the width of the beam's web, and d is the distance from extreme compression fibre to the centroid of tensile reinforcement. (2) The CFRP percentage was obtained from $\rho_f = ((2 \times a_f \times b_f) / (b_w \times s_f \times \sin \theta_f)) \times 100$ where a_f and b_f are the dimensions of the laminate cross section, and s_f is the CFRP spacing. (3) The percentage of the vertical steel stirrups was obtained from $\rho_{sw} = (A_{sw} / (b_w \times s_w)) \times 100$ where A_{sw} is the cross sectional area of the arms of a steel stirrup, and s_w is the spacing of the stirrups.

The three point beam bending tests (Fig. 1) were carried out using a servo closed-loop control equipment, taking the signal read in the displacement transducer (LVDT), placed at the loaded section, to control the test at a deflection rate of 0.01 mm/second. With the purpose of obtaining the strain variation along two laminates that have the highest probability of providing the largest contribution for the shear strengthening of the RC beam, four strain gauges (SG_L) were bonded in each inclined laminate, and three SG_L were bonded in each vertical laminate according to the arrangement represented in Fig. 3. Adopting the same principle, one steel stirrup was monitored with three strain gauges (SG_S) installed according to the configuration represented in Fig. 4. The location of the monitored laminates and stirrups in the NSM shear strengthened beams is represented in Fig. 5.

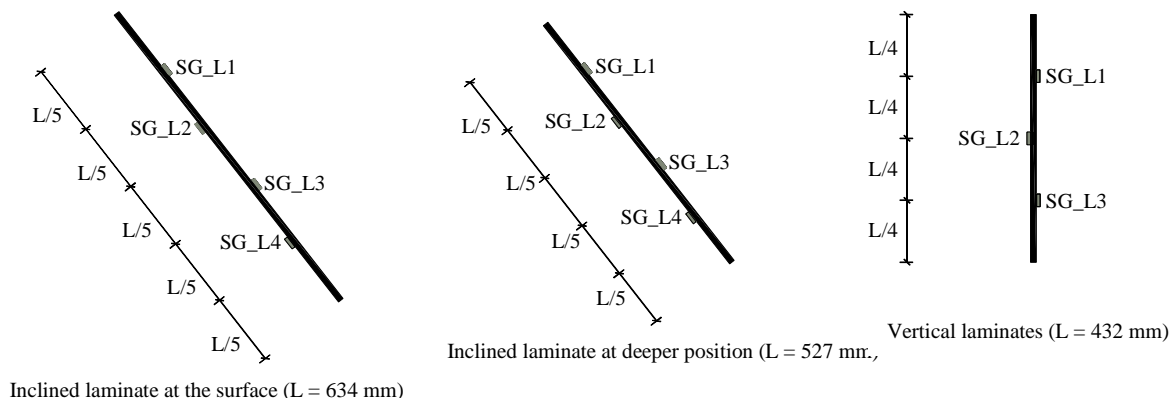


Figure 3: Position of the strain gauges in the CFRP laminates (dimensions in mm).

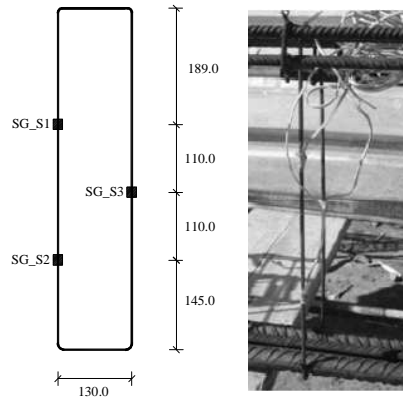


Figure 4: Position of the strain gauges in the steel stirrups (dimensions in mm).

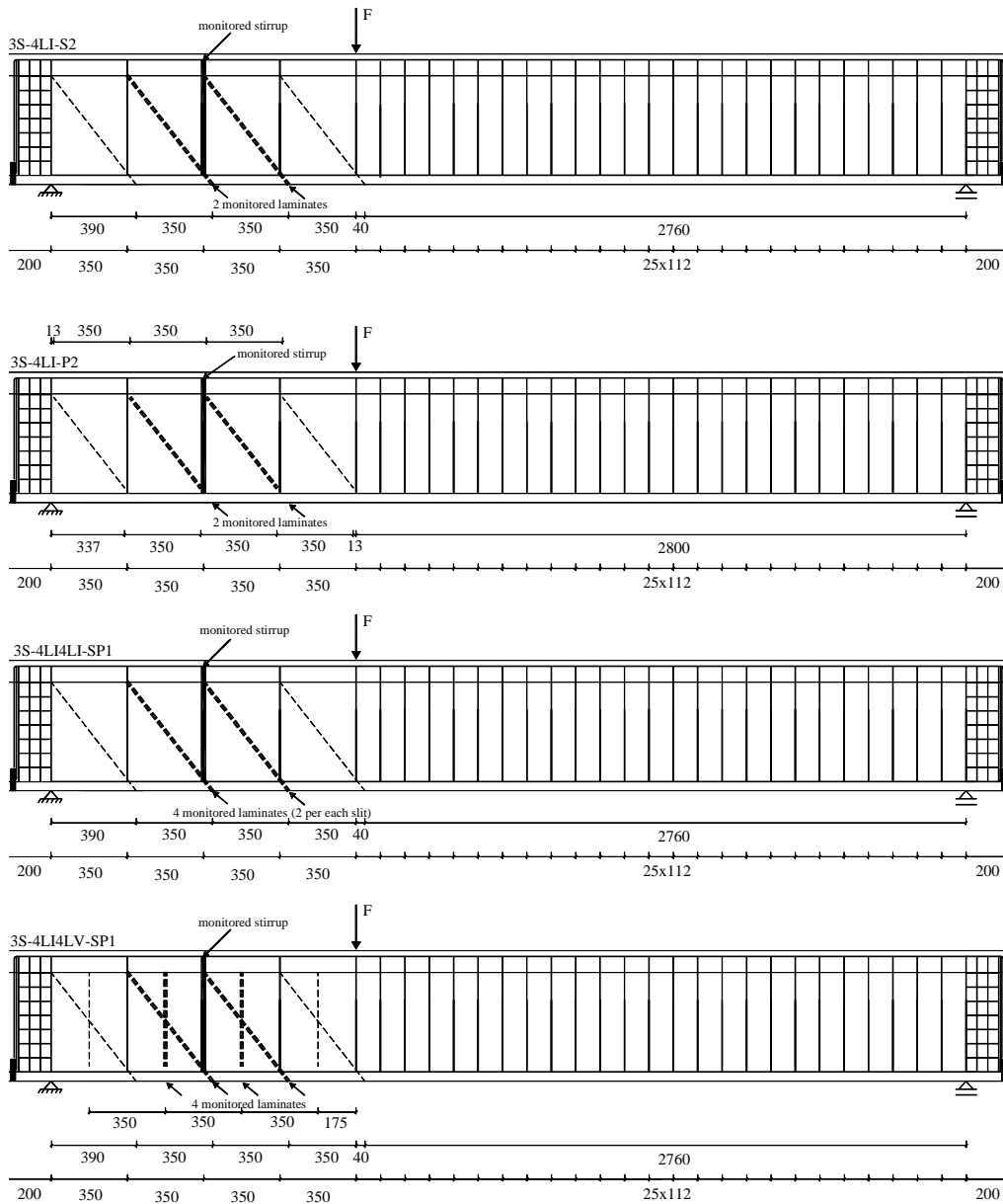


Figure 5: Localization of the monitored CFRP laminates and steel stirrups in the tested beams (dimensions in mm).

3. EXPERIMENTAL RESULTS AND ANALYSIS

The relationship between the applied force and the deflection at the loaded section (u_{LS}) for the tested beams is represented in Fig. 6a. This figure shows that ΔF represents the increase of the load provided by a shear strengthening system, while F^{3S-R} is the load capacity of the 3S-R reference beam. The $\Delta F/F^{3S-R}$ ratio was evaluated for deflections greater than the corresponding to the formation of the first shear crack in the 3S-R reference beam, and the $\Delta F/F^{3S-R}$ vs u_{LS} relationship is depicted in Fig. 6b.

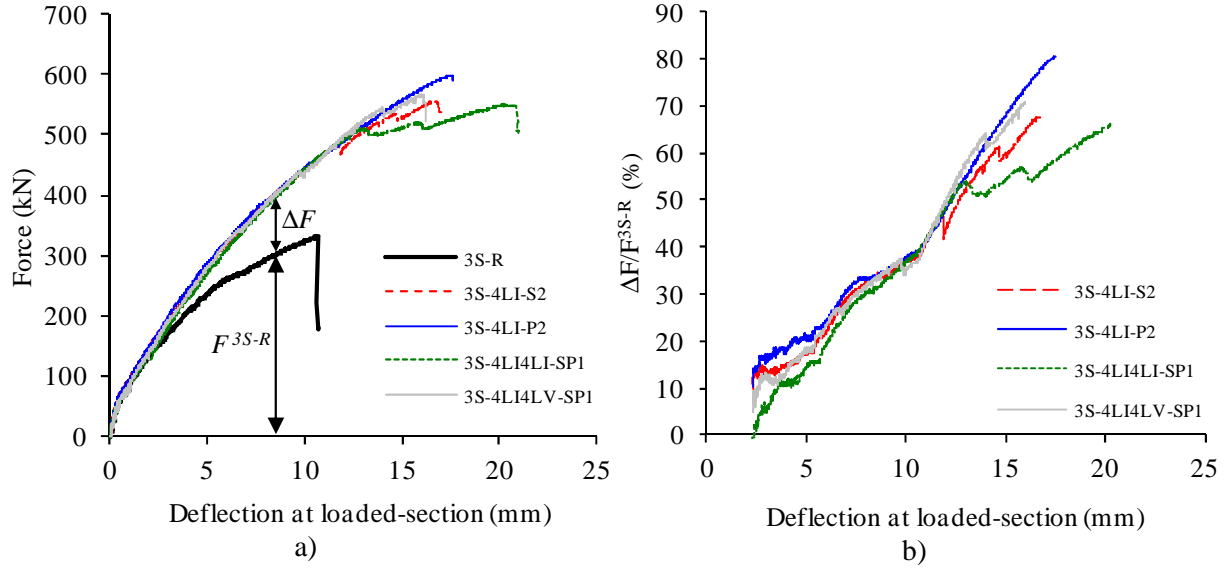


Figure 6: Force versus deflection at loaded section of the tested beams.

Assuming that $\Delta F_{max} = F_{max} - F_{max}^{3S-R}$, being F_{max}^{3S-R} and F_{max} the load carrying capacity (maximum force) of the reference beam (3S-R) and of the shear strengthened beam, respectively, the $\Delta F_{max}/F_{max}^{3S-R}$ ratio was also evaluated. The values for F_{max} , $\Delta F_{max}/F_{max}^{3S-R}$, and the deflection at loaded section corresponding to F_{max} ($u_{F_{max}}$) are included in Table 2.

Table 2: Experimental results of the tested beams.

Beam	F_{max} [kN]	$\Delta F_{max}/F_{max}^{3S-R}$ [%]	F_{max}/F_{max}^{3S-R}	$u_{F_{max}}$ [mm]
3S-R	331.4	0.0	1.00	10.68
3S-4LI-S2	555.5	67.6	1.68	16.66
3S-4LI-P2	598.6	80.6	1.81	17.45
3S-4LI4LI-SP1	550.1	66.0	1.66	20.26
3S-4LI4LV-SP1	566.4	70.9	1.71	15.97

It is verified that $\Delta F_{max}/F_{max}^{3S-R}$ has varied between 66% and 81%, which is higher than the load carrying increase levels registered in previous experimental programs with NSM CFRP shear strengthening configurations applied in T cross section RC beams [3]. The deflection at maximum load, $u_{F_{max}}$, was also larger in all the strengthened beams than in the reference beam. The maximum value of the ratio $\Delta F_{max}/F_{max}^{3S-R}$ was recorded in 3S-4LI-P2 beam, which evidences the benefits of applying the laminates as deepest as possible into the beam's web. However, this configuration was not the most suitable for seismic retrofitting, since the laminates have not a proper inclination for the shear forces that can occur in inverse orientation (upward loading). The shear configuration applied in

the 3S-4LI4LV-SP1 beam is more suitable for this type of loading conditions, and a significant increase of load carrying capacity was also obtained for this strengthening arrangement (71%).

Table 3 includes the strains measured in the monitored laminates at F_{max} , $\epsilon_{CFRP}^{SG_Li}$ ($i=1$ to 4 for the inclined laminates and $i=1$ to 3 for vertical laminates, see Fig. 3), and the maximum strain in these laminates up to F_{max} , ϵ_{CFRP}^{max} . It is verified that the ϵ_{CFRP}^{max} varies between 12.2 ‰ and 16.3 ‰, which is higher than 69% of the ultimate strain of the adopted CFRP laminates, justifying the high strengthening effectiveness provided by the adopted configurations. Comparing the strains in the laminates at different depth it seems do not have a clear tendency of an increase of the strains with the deeper position of the laminate, since the strains are more dependent of the relative distance between the SG and the shear failure crack crossing the laminate. However, the maximum average value of the $\epsilon_{CFRP}^{SG_Li}$ was recorded in the laminate B (positioned at deeper position) of 3S-4LI4LI-SP1 beam (11.3 ‰). According to the maximum strain values recorded in the strain gauges applied in the monitored steel stirrup, when the maximum load of the strengthened beams was attained the stirrup crossed by the shear failure crack was already yielded.

Table 3: Strain values in the CFRP laminates.

Beam	CFRP ⁽¹⁾	$\epsilon_{CFRP}^{SG_L1}$ [‰]	$\epsilon_{CFRP}^{SG_L2}$ [‰]	$\epsilon_{CFRP}^{SG_L3}$ [‰]	$\epsilon_{CFRP}^{SG_L4}$ [‰]	ϵ_{CFRP}^{max} [‰]
3S-4LI-S2	A	10.15	16.33	9.91	0.13	16.33
	B	0.30 (0.30)	7.21 (7.37)	8.19 (8.62)	4.80 (6.65)	
3S-4LI-P2	A	12.35	13.70	12.49	0.24	13.70
	B	0.17	0.27	3.84	4.55	
3S-4LI4LI-SP1	A	5.33 (6.29)	7.63	11.46	8.60	14.28
	B	13.31	14.28	10.11	3.69 (5.67)	
	A ⁽²⁾	6.55	7.37	12.28	9.37	
	B ⁽²⁾	11.32	12.99	12.46	8.78	
3S-4LI4LV-SP1	A	11.27	11.59	10.71	9.23	12.24
	B	0.21	7.21	8.85	6.75 (9.30)	
	A ⁽³⁾	2.81	12.24	8.47	Not exist.	
	B ⁽³⁾	0.57	6.89	10.81	Not exist.	

(1) The CFRP A was the closest to the loaded section. (2) Deeper laminate. (3) Vertical laminate.

Note: The strain values in brackets are referred to the load, at which occurred the maximum strain in the laminates before the maximum load.

Figure 7 represents the crack patterns at failure of the tested beams. As expected, all the tested beams failed in shear. In the beam strengthened with laminates of a cross section depth of 20 mm (3S-4LI-S2 and 3S-4LI-P2), the failure was quite violent, since the laminates have ruptured. The beams strengthened with laminates of a cross section depth of 10 mm (3S-4LI4LI-SP1 and 3S-4LI4LV-SP1) the laminates have not ruptured, which has contributed for a pseudo-ductility in the post-peak phase of the response of these beams, due to the progressive debond of these laminates. In fact, at a deflection of about 27 mm, the 3S-4LI4LI-SP1 beam presented a load carrying capacity of 468 kN, which is 85% of the maximum load (F_{max}). This deflection level was 33% higher than the deflection at F_{max} (20.3 mm). For a deflection of about 22.2 mm the 3S-4LI4LV-SP1 beam presented a load carrying capacity of 486 kN (85% of F_{max}). This deflection level was 39% higher than the deflection at F_{max} (16 mm) of this beam. In the following paragraph a deeper analysis is executed on the crack propagation and crack pattern at failure of the tested beams.

In the 3S-4LI-S2 beam, at a load level of about 530 kN the third laminate from the loaded section failed at its bottom part (Fig. 7a), with a formation of a concrete volume surrounding the laminate.

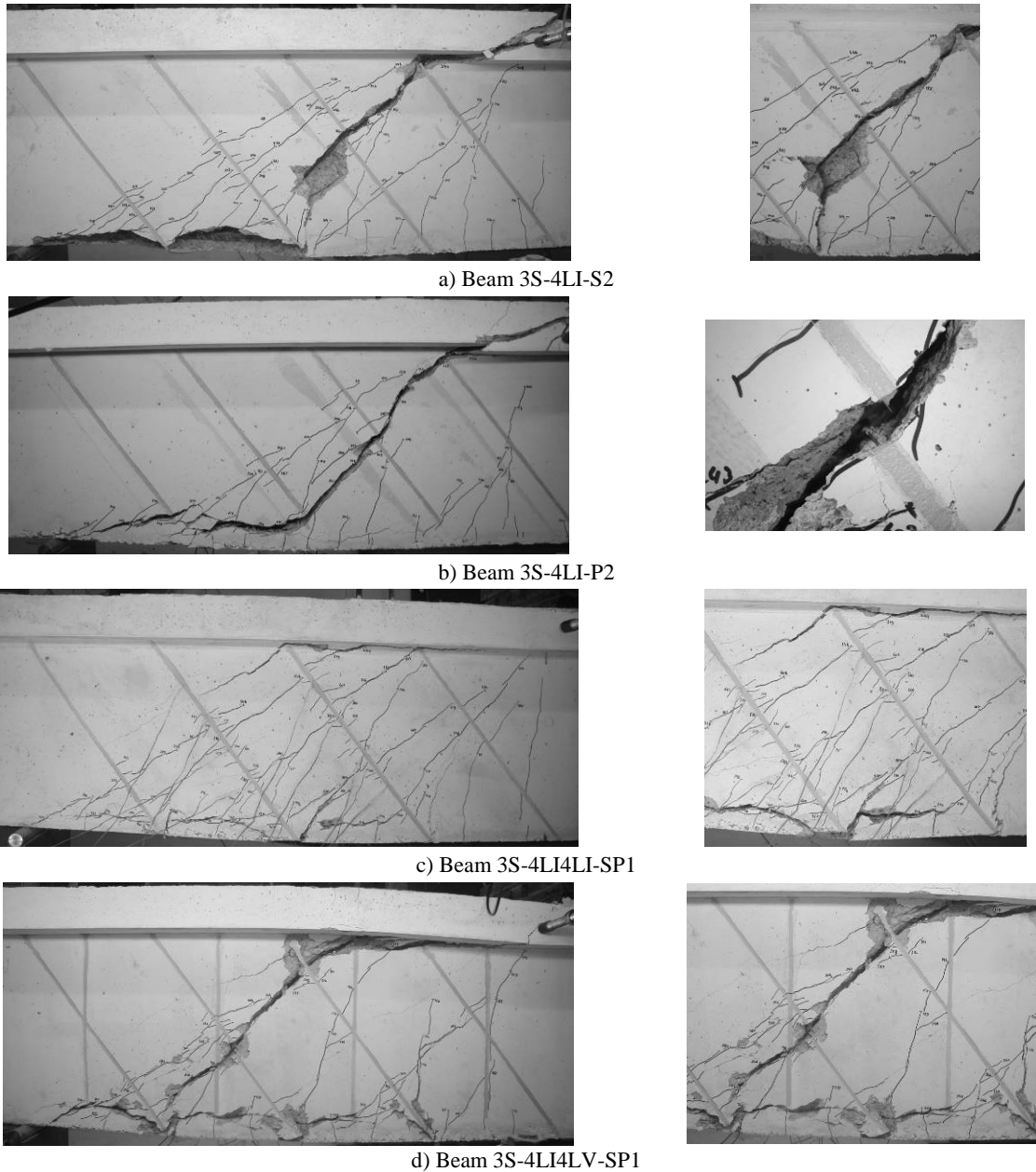


Figure 7: Crack patterns of the tested beams at failure.

This was followed by a decay of the load carrying capacity of this beam (Fig. 6a). The load was transferred, mainly, to the second laminate from the loaded section, and the load was again increased up to the moment when this laminate has ruptured, followed by sudden and abrupt load decay. In case of 3S-4LI-P2, after the formation of inclined shear cracks crossing the laminates, cracks started progressing along a plane located between the longitudinal tensile steel bars and the bottom extremities of the two laminates closest to the support (Fig. 7b), and then getting an inclination in direction to the top extremity of the first laminate from the load section, by crossing the second laminate at its intermediate length. The maximum load coincided with the rupture of this second laminate from the loaded section. Like the previous one, this rupture was also quite violent. In the 3S-4LI4LI-SP1 beam, the failure cracks progressed mainly just below the extremities of the laminates, and no laminate has ruptured, which justifies the smallest load carrying capacity of this strengthened beam. However, the high level of strains recorded in the monitored laminates indicates that before the localization of the failure cracks the laminates were very effective in limiting the propagation of the shear cracks. Finally, in the 3S-4LI4LV-SP1 beam no laminate has ruptured up to peak load, and two failure cracks were formed, one progressing at the interface web/flange along the first two inclined and vertical laminates from the loaded section, and then inflecting up to the bottom extremity of the

inclined laminate closest to the support, by crossing the third inclined and vertical laminates from the loaded section. The other failure crack progressed along a plane between the longitudinal tensile steel bars and the bottom extremities of the three inclined and vertical laminates from the support of the beam. The option for having two independent laminates in each slit, such is the case of 3S-4LI4LI-SP1 beam, has conducted to a more ductile behaviour after peak load, indicating that, after the failure of the laminates positioned closest to the surface, the laminates deeper positioned into the groves have provided a reserve of load carrying capacity (Fig. 8).

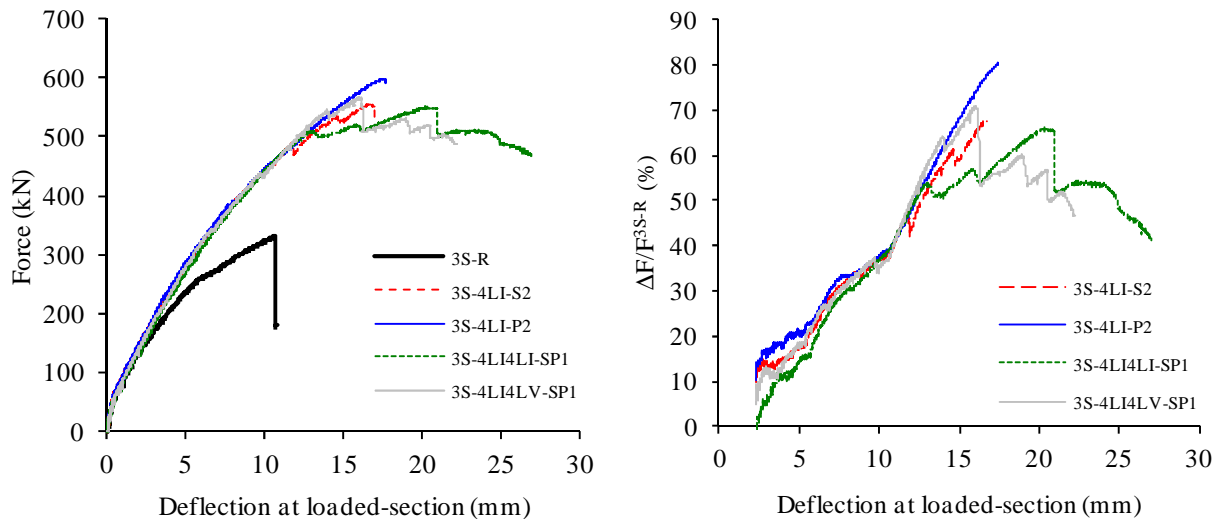


Figure 8: Influence of the depth installation of the CFRP laminate on the load-deflection behaviour.

5. CONCLUSIONS

Available reliable theoretical models for the prediction of the contribution of NSM CFRP laminates for the shear strengthening of RC beams, and data obtained from pullout tests, have indicated that the application of the laminates as deeper as possible into the web of the beam may be more effective since during the pullout process of a laminate crossed by a shear failure crack a larger fracture area is mobilized associated to the tensile fracture failure mode occurred in this process. This was the fundamental motivation of the experimental program carried out, composed of T cross section RC beams of relatively high cross section height, where laminates were positioned at different depth into slits opened at the lateral faces of the beam's web. From the obtained experimental results it can be concluded that NSM shear strengthening technique with CFRP laminates is very effective in RC beams of relatively high cross section height not only in terms of increasing the load carrying capacity of the beams, but also in assuring higher mobilization of the tensile properties of the CFRP. The obtained results also indicated that as deeper the laminates are installed into the beam's web as higher is the shear strengthening effectiveness they can provide. The option for having two independent laminates in each slit, or the use of CFRP configurations with two kinds of inclinations for the laminates installed at different depth inside the slit has provided a more ductile behaviour after peak load for the NSM shear strengthened beams.

ACKNOWLEDGMENTS

The authors wish to acknowledge the support provided by the "Empreiteiros Casais", S&P - Clever Reinforcement Ibérica and Secil (Unibetão, Braga). The study reported in this paper is part of the research project PTDC/ECM/114511/2009, supported by the Portuguese Foundation for Science and Technology (FCT).

REFERENCES

- [1] Kotynia, R., "Shear strengthening of RC beams with NSM CFRP laminates", 8th International Symposium on Fiber Reinforced Polymer Reinforcement for Concrete Structures (FRPRCS-8), Patras, Greece, July (2007).
- [2] El-Hacha, R. and Wagner, M., "Shear Strengthening of Reinforced Concrete Beams using Near-Surface Mounted CFRP Strips", 9th International Symposium on Fiber Reinforced Polymers Reinforcement for Concrete Structures (FRPRCS-9), Sydney, Australia, July, 10 pp. (2009).
- [3] Dias, S.J.E.; Barros, J.A.O., "Shear strengthening of RC beams with NSM CFRP laminates: experimental research and analytical formulation", accepted to be published in the Composite Structures Journal, 2013.
- [4] Bianco, V., Barros, J.A.O., Monti, G., "Three dimensional mechanical model for simulating the NSM FRP strips shear strength contribution to RC beams", Engineering Structures Journal, 31(4), 815-826, April 2009.
- [5] Costa, I.G. and Barros, J.A.O., "Assessment of the bond behavior of NSM FRP materials by pullout tests", First Middle East Conference on Smart Monitoring, Assessment and Rehabilitation of Civil Structures, Dubai, 8-10 February (2011).
- [6] Collins, M. P., and Mitchell, D., "Prestressed Concrete Structures", Prentice-Hall, Inc., Englewood Cliffs, New Jersey (1997).
- [7] ISO 527-5, "Plastics - Determination of tensile properties - Part 5: Test conditions for unidirectional fibre-reinforced plastic composites", International Organization for Standardization (ISO), Geneva, Switzerland, 9 pp. (1997).
- [8] Costa, I.G.; Barros, J.A.O., "Assessment of the long term behavior of structural adhesives in the context of NSM flexural strengthening technique with prestressed CFRP laminates", submitted to FRPRCS11, Guimarães, 2013.
- [9] ISO 527-2, "Plastics - Determination of tensile properties - Part 2: Test conditions for moulding and extrusion plastics" International Organization for Standardization, 1993.